



Research Article

Crystallization of Lysozyme on Metal Surfaces Using a Monomode Microwave System

Kevin Mauge-Lewis¹, Brittney Gordon¹, Fareeha Syed¹, Saarah Syed¹, Enock Bonyi¹
Muzaffer Mohammed¹, Eric A. Toth^{2,3}, Dereje Seifu⁴, Kadir Aslan¹✉

¹Morgan State University, Department of Chemistry, 1700 East Cold Spring Lane, Baltimore, MD 21251, USA.

²University of Maryland at Baltimore, Department of Biochemistry and Molecular Biology, 9600 Gudelsky Drive, Rockville, MD 20850, USA.

³Marlene and Stewart Greenebaum Cancer Center, University of Maryland School of Medicine, Baltimore, Maryland 21201, USA.

⁴Morgan State University, Department of Physics, 1700 East Cold Spring Lane, Baltimore, MD 21251, USA.

✉ Corresponding author: E-mail: kadir.aslan@morgan.edu

Received: Mar. 15, 2016; **Accepted:** Apr. 11, 2016; **Published:** Apr. 28, 2016.

Citation: Kevin Mauge-Lewis, Brittney Gordon, Fareeha Syed, Saarah Syed, Enock Bonyi, Muzaffer Mohammed, Eric A. Toth, Dereje Seifu and Kadir Aslan. Crystallization of Lysozyme on Metal Surfaces Using a Monomode Microwave System. *Nano Biomed. Eng.*, 2016, 8(2): 60-71.

DOI: 10.5101/nbe.v8i2.p60-71.

Abstract

The effect of metal surfaces on the crystallization of lysozyme using the Metal-Assisted and Microwave-Accelerated Evaporative Crystallization (MA-MAEC) technique and a monomode microwave system is described. Our microwave system (is called the iCrystal system hereafter for brevity) is comprised of a 100 W variable power monomode microwave source, a monomode cavity, fiber optic temperature probes and digital cameras. Crystallization of lysozyme (a model protein) was conducted using the iCrystal system on four different types of circular crystallization plates with 21-well sample capacity (i.e., crystallization plates): (i) blank: a continuous surface without a metal, (ii) silver nanoparticle films (SNFs): a discontinuous metal film, (iii) iron nano-columns: a semi-continuous metal film, and (iv) indium tin oxide (ITO): a continuous metal film. Lysozyme crystals grown on all crystallization plates were characterized by X-ray crystallography and found to be X-ray diffraction quality. The use of iron nano-columns afforded for the growth of largest number of lysozyme crystals with a narrow size distribution. ITO-modified crystallization plates were deemed to be best of all the crystallization plates based on the observations that lysozyme crystals were grown at the shortest time (370 ± 36 minutes) with a narrow size distribution up to 460 nm in size.

Keywords: Protein Crystallization; iCrystal System; Metal-Assisted and Microwave-Accelerated Evaporative Crystallization; Iron Nano-Columns; Silver Island Films; Indium Tin Oxide

Introduction

The growth of biological macromolecule crystals continues to attract the interest of researchers worldwide due to its numerous implications in the medical and pharmaceutical fields. Current interest is in the control over the crystallization of proteins in terms

of speed of crystallization, size and quality of crystals, which is still largely empirical and operator-dependent [1]. Subsequently, a plethora of crystallization techniques were developed [2]-[6]. These techniques aim to shorten the time of crystallization and/or grow X-ray diffraction quality protein crystals to obtain structural information about the protein, which can be

used in the development of new drugs and therapies for human diseases [7].

As the field of crystallography continues to advance, allowing researchers to obtain a more comprehensive understanding of protein crystallization, new approaches that involve the incorporation of materials research, nanoscience and molecular biotechnology are being introduced [8]. For example, polymeric films containing ionizable groups, such as sulfonated polystyrene, have been tested as heterogeneous nucleation inducing surfaces for proteins, among other numerous materials and native and/or engineered surfaces [9]-[11]. Nucleation kinetics and thermodynamics studies indicated that significant conformational changes can occur as the protein interacts with these surfaces [10, 12]. Recently, the use of nucleation agents to accelerate the crystallization of proteins was demonstrated [13]. In addition, protein modeling techniques to capture kinetics and thermodynamics of the crystallization on such surfaces on the colloidal scale are being developed [14]-[16]. Despite the developments summarized above, there is a continuous need for detailed investigation of surfaces that are ideal for the growth of diffraction quality protein crystals in a rapid manner.

The Aslan Research Group previously proposed that the MA-MAEC technique can be used for the rapid crystallization of biological and chemical materials using a number of metallic materials, such as, silver, gold, copper and aluminum and other metal oxides deposited on non-metallic surfaces [17]. Subsequently, we experimentally demonstrated the rapid crystallization of amino acids and drug molecules on surfaces modified with silver nanoparticles using the MA-MAEC technique to date. Our initial experimental results indicated that the use of chemically deposited silver island films (a dis-continuous silvered surface) resulted in the rapid growth of crystals in conjunction with microwave heating [18, 19, 3, 20, 21, 22]. In addition, we also demonstrated the proof-of-principle of the MA-MAEC technique for the crystallization of lysozyme using SNFs and a 700 W conventional microwave cavity [23]. These results demonstrated that the use of a conventional microwave oven with a multimode source and a duty cycle afforded for the crystallization of lysozyme up to 4-fold faster than at room temperature (no microwave heating) [23]. However, the use of a conventional microwave oven that only has a full power output (e.g., 700 W, no true control of microwave power) to accelerate the growth

of lysozyme crystals decreased quality of the crystals grown on SNFs [23]. These observations have led us to further optimization of the MA-MAEC technique for the crystallization of proteins by using different the metal surfaces (instead of silver) and a monomode microwave system (instead of multimode system).

In this study, we investigated crystallization of lysozyme (as a model protein) on three different metal surfaces to determine the optimal surfaces for the crystallization of proteins using the MA-MAEC technique and the iCrystal system (a mono-mode solid state microwave source with a variable power up to 100 W and a monomode microwave cavity with transverse electric mode, TE_{10}). The present study yielded the following advancements in protein crystallization: 1) the use of the MA-MAEC technique with the iCrystal system significantly reduces the amount of time required for growth of lysozyme crystals; 2) X-ray diffraction quality protein crystals can be grown by continuous microwave heating; 3) silver, iron and ITO nanoparticle surfaces can be used to control the growth, size and number of the crystals; and 4) ITO is the most efficient surface for the growth of lysozyme using iCrystal system and the MA-MAEC technique to date.

Materials and Methods

Materials

Materials were purchased and utilized as described in our previously published work [23]. Lysozyme (lyophilized from chicken egg-white) and lysozyme crystallization reagent (30% w/v polyethylene glycol monomethyl ether 5000, 1.0 M sodium chloride, and 0.05 M sodium acetate trihydrate pH 4.6) were all purchased from Hampton Research (Aliso Viejo, CA, USA), and was used as received. Poly(methyl methacrylate) (PMMA) disks (5 cm in diameter) were purchased from McMaster-Carr (Elmhurst, IL, USA) and silicone isolators (21 wells, 2.0 mm depth X 4.5 mm diameter) were purchased from Grace Biolabs (Bend, OR, USA). Ethanol 190 proof (95%) was purchased from Pharmco Products Inc. An EMS 150R S sputter coater and silver targets (57 mm in diameter) were purchased from Electron Microscopy Sciences (Hatfield, PA, USA). A R&D magnetron sputtering source and iron oxide targets were purchased from the Kurt J. Lesker Company (Jefferson Hills, PA, USA). ITO-coated PET films (ITO = 115 nm thick, PET: thickness = 0.175 mm, width = 300 mm, length = 1 m)

were purchased from the MTI Corporation (Richmond, CA, USA). A FISO UMI4 Universal Multichannel Instrument was purchased from FISO Technologies (Quebec, QC, Canada). All aqueous solutions were prepared using deionized water ($> 18.0 \text{ M}\Omega \cdot \text{cm}$ resistivity at 25°C) obtained from Millipore Direct Q3 system except stated otherwise.

Methods

(1) Preparation of lysozyme stock solution.

Lysozyme solutions were prepared as described in our previously published work [23]. In short, lysozyme powder (60 mg) was dissolved in 1.0 mL of sodium acetate solvent (pH 4.6) and was mixed with 500 μL of crystallization reagent in a clean glass vial. The crystallization solution was later extracted using a sterile syringe (0.8 mm x 40 mm) and then slowly filtered back into the vial through a sterile syringe filter (ValuPrep, 25 mm cellulose acetate, 0.2 μm). [Note: all crystallization solution used in this work was colorless, transparent, and contained no undissolved particles and foam].

(2) Preparation of SNFs-coated crystallization plates. Silver nanoparticle films (SNFs, 1 nm thick)-deposited and blank crystallization plates were prepared as previously described in our other published work [3]. [Note: All PMMA disks were cleaned for 1 min using Harrick plasma cleaner PDC-32G (Ithaca, NY, USA) before preparation and use]. Subsequently, 21-well silicone isolators were placed securely on top of the crystallization plates, which afforded us the ability to conduct multiple crystallization experiments on a single crystallization plate. In addition, polymer transparent cover was then placed on top of all crystallization plates before the commencement of crystallization experiments.

(3) Preparation of iron nano-columns coated crystallization plates. Iron nano-columns (height: 50 nm, 100 nm and 200 nm) were deposited onto the blank crystallization plates using DC/RF magnetron sputtering AXXIS tool (from Kurt J. Lesker Company, USA) with Fe target of purity 99.9% at an angle of 70° in order to create a roughened and semi-continuous film. Subsequently, 21-well silicone isolators were positioned securely on top of the crystallization plates and a transparent polymer cover was then placed on top of each of the crystallization plates before the commencement of the crystallization experiments.

(4) Preparation of ITO-modified crystallization

plates. ITO surfaces (5 mm in diameter) were punched from the ITO-coated PET films and positioned in alignment with each of the individual 21-wells of the silicone isolator. The 21-well silicone isolators with the attached ITO dots were subsequently positioned onto the blank crystallization plates. A transparent polymer covering was positioned on top of each of the crystallization plates before the commencement of the crystallization experiments.

(5) Crystallization of lysozyme using the iCrystal system. The crystallization experiments were conducted using the four different crystallization plates with the following surface modifications: (i) no modification (i.e., blank a control surface), (ii) SNFs, (iii) iron nano-columns and (iv) ITO. In a typical crystallization experiment using the crystallization plates, 15 μL of the stock lysozyme solution was placed into each of the 21 wells of the crystallization plates. On the ITO-modified crystallization plates, only 8.0 μL of the prepared solution was placed into each individual well of the silicone isolator. Crystallization of the lysozyme was performed via a continuous heating cycle at 70 W of power on each of the plates.

(6) Characterization of lysozyme crystals. Optical images of the growth of lysozyme crystals on the crystallization plates were recorded every 15 minutes (by stopping the microwave heating for 30 seconds) using a Swift Digital M10L monocular light microscope at time intervals of at 10X magnification and using the Motic Images 2.0 software. Measurements of crystal size were also carried out in micrometers and the average size growth progression of the lysozyme crystals was calculated with ImageJ (Image Processing and Analysis in Java) software.

(7) Temperature measurements. Real-time temperature measurements inside the iCrystal system were carried out using a FISO multichannel fiber optic sensors. Monomode cavity contains nine observation ports (arranged by 3x3) to facilitate capturing of images and monitoring temperature. Two fiber optic sensors were used to collect temperature data at two locations 1) temperature of the solvent in well and 2) temperature of the interior environment of the cavity.

(8) XRD analysis of lysozyme crystals. All XRD measurements were performed as previously described [23] at the W.M. Keck/NIST X-ray Crystallography Core Facility at the Institute for Bioscience and Biotechnology Research, University of Maryland School of Medicine, Rockville, Maryland. Prior

to data collection, crystals were transferred into a modified mother liquor composed of the crystallization buffer with the exception that polyethylene glycol monomethyl ether 5000 is replaced with polyethylene glycol 400 at a final concentration of 30% (v/v). Lysozyme crystals were flash cooled under liquid nitrogen prior to data collection at 100 K. The morphology of the crystals was primitive tetragonal ($P4_32_12$) and contained a monomer in the asymmetric unit. X-ray diffraction data was later collected using an X-ray generator (MicroMax 7, Rigaku/MS, The Woodlands, TX) and a Raxis4++ image plate detector (Rigaku/MS). Each data set was collected at the crystal-to-detector distance (120.1 mm), with the exposure time (1 minute), oscillation angle (0.5°), and oscillation range (61.0°). The images were processed and scaled using iMOSFLM [24] and Aimless [25] from the CCP4 [26] program suite.

Results and Discussion

Figure 1(a) shows the real-color photographs of the

iCrystal system and its four major components: (i) a FISO multichannel temperature measuring instrument, (ii) a solid state, variable power monomode microwave generator, (iii) a monomode microwave cavity, and the (iv) an crystallization plate. The iCrystal system affords for the rapid crystallization of the lysozyme protein through the utilization of continuous and low-wattage microwave heating, the circular crystallization plate design and metal nanoparticles. Figure 1(b) displays the real-color photographs of the four different crystallization plates that are utilized for the crystallization of the lysozyme: (i) blank crystallization plates (continuous surface without metal), (ii) SNFs-modified crystallization plates (discontinuous metal film), (iii) iron nano-columns deposited crystallization plates (roughened semi-continuous metal films) and (iv) ITO-modified crystallization plate (continuous metal film). Each of these crystallization plates were affixed with a 21-well silicone isolator and each well has a sample capacity of $30\ \mu\text{L}$. Additionally, the placement of a thin polymer cover on top of the silicone isolators prevents the evaporation of the solvent during the

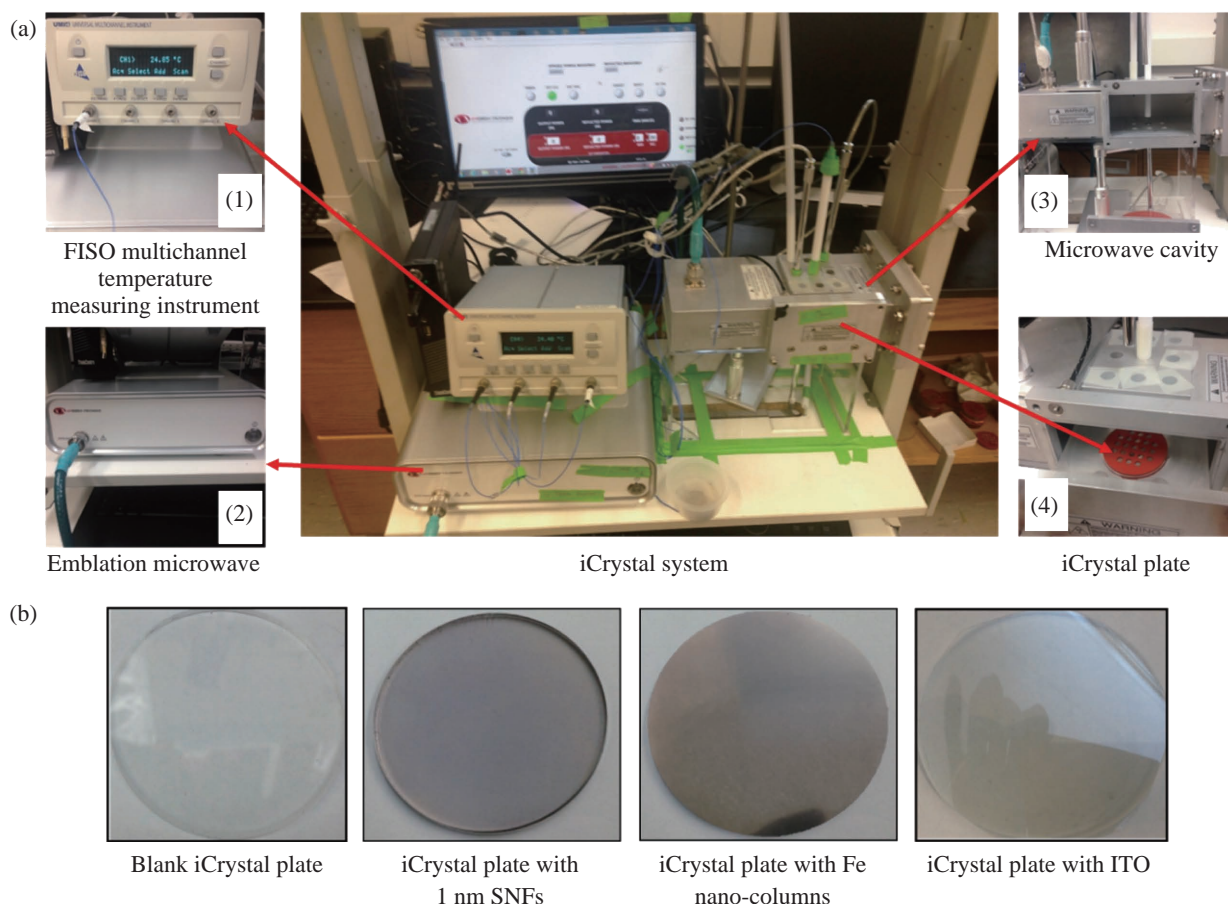
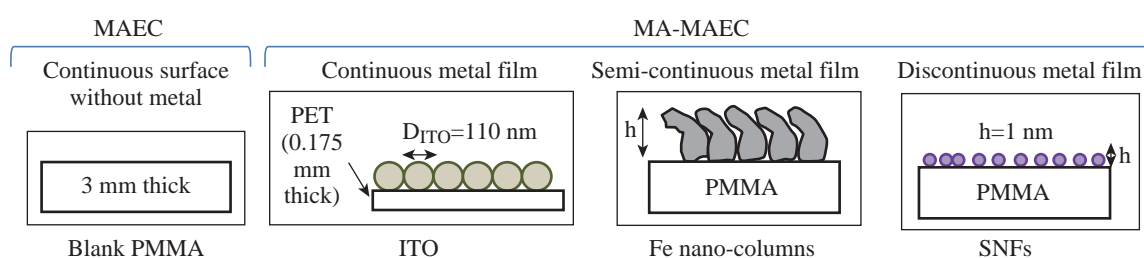


Fig. 1 (a) Real-color photograph of the iCrystal system and four major components: (1) Fiso Multichannel temperature measurement instrument, (2) monomode microwave source (2.45 GHz, up to 100 W), (3) monomode microwave cavity, and (4) iCrystal plates. (b) Real-color photographs of the four different crystallization plate surfaces utilized for the experiments.

Table 1 Summary of results for the crystallization of lysozyme from 60 mg/mL solution on crystallization plates using the MA-MAEC technique with continuous heating at 70 W of power. Experiments were repeated three times at each condition.

iCrystal system at 70 W	Initial crystallization time* (minutes)	Crystallization time** (minutes)	Size range (min-max) (μm)	Average number of crystals***
Blank PMMA	<15	555 ± 77.0	43.0 – 268	305 ± 49.0
ITO	<15	370 ± 36.0	56.0 – 584	73 ± 13.0
Fe (50 nm)	<15	510 ± 45.0	26.0 – 262	461 ± 83.0
Fe (100 nm)	<15	845 ± 22.0	18.0 – 347	286 ± 42.0
Fe (200 nm)	<15	810 ± 51.0	42.0 – 460	111 ± 26.0
SNFs (1 nm)	<15	527 ± 28.0	41.0 – 248	435 ± 117



SNFs: Silver nanoparticle films (1 nm thick) on crystallization plates.

Blank PMMA: crystallization plates without SNFs.

Fe: Iron Nano-columns.

ITO: Indium Tin Oxide.

* Initial crystallization time refers to the time of appearance of first crystal detectable by our optical microscope).

** Crystallization time refers to the time when lysozyme crystals stopped their growth.

*** Average number of all observable crystals counted on crystallization plates with 21-wells.

nucleation and growth stages and potential denaturation of the protein as a result of the microwave heating.

Table 1 provides the summary of the results obtained for the crystallization of lysozyme performed on crystallization plates using the MA-MAEC technique at 70 W of continuous microwave heating. On each crystallization plate, lysozyme crystals were observed after the first 15 minute interval of microwave heating. In this regard, initial crystallization is reported to have taken place during a time frame before the 15 minute heating interval was completed. In order to compare the effectiveness of all crystallization plates for the crystallization of lysozyme, the average time necessary for the complete crystallization of lysozyme (the time when lysozyme crystals stopped growing) to occur on crystallization plates was recorded ($n = 3$, at least three different repetitions of each experimental condition). The average crystallization time for lysozyme crystals grown on crystallization plates: blank, SNFs-deposited, iron nano-columns deposited and ITO-modified was 555 ± 77 minutes, 527 ± 28 minutes, 510 ± 45 minutes and 370 ± 36 minutes, respectively. These observations imply that metal nanoparticles serve to decrease the

amount of time needed for the complete crystallization of the lysozyme on crystallization plates using the MA-MAEC technique and iCrystal system. It is important to comment on the choice for 70 W power setting in the iCrystal system, where one can vary the microwave power between 0 - 100 W. The initial results for the crystallization of lysozyme using various microwave power (Table S1) show that 70 W power setting afforded for the fastest crystallization times on blank and SNFs-deposited crystallization plates. Subsequently, the remainder of this investigation was carried out using 70 W power setting on the iCrystal system.

The type of metal nanoparticles used and the surface feature of the crystallization plates clearly have an effect on the size distribution and the average number of crystals that are grown on the crystallization plates. For example, lysozyme crystals grown on the blank and SNFs-deposited plates had comparable size range distributions, where the size of lysozyme crystals were in the ranges of 43 – 268 μm and 41 – 248 μm , respectively. However, the SNFs-deposited plate produced a greater number of lysozyme crystals

(435 ± 117), when compared to the number of crystals grown on the blank plates (305 ± 49). The increase in the number of lysozyme crystals can be attributed to the presence of the silver nanoparticles on the surface of the crystallization plate serving as selective nucleation sites for lysozyme. Since lysozyme crystals can nucleate faster on metal nanoparticles (due to chemical interactions between primary amine and sulfhydryl groups of the proteins and metals) than on the blank crystallization plate that contains no metal nanoparticles, lysozyme crystals can grow larger in size and in numbers. Figures S1 and S2 (in Supporting Information) display the time progression of the growth of lysozyme crystals on the blank crystallization plates and the SNFs-deposited crystallization plates, respectively. These results show that one can grow lysozyme crystals of ~ 100 nm in size after 300 min on blank crystallization plates and after 150 min on SNFs-deposited crystallization plates, which demonstrates the advantage of using SNFs for the crystallization of lysozyme.

To further investigate the effect of surface features of the crystallization plates on the growth of lysozyme crystals crystallization plates with iron nano-columns (semi-continuous metal films) and ITO (continuous metal films) were employed. Iron nano-columns (height of ~ 50 , 100 and 200 nm, roughness increases as the thickness increases) are deposited as a roughened semi-continuous films on crystallization plates as revealed by SEM images (Figure S3). In this regard, the average time for complete crystallization of the lysozyme to occur on the crystallization plate containing the iron nano-columns with 50 nm height (510 ± 45.0 minutes) was similar that for the blank and SNFs-deposited crystallization plates. Additional crystallization experiments carried out on iron nano-columns at heights of 100 nm and 200 nm revealed that the complete crystallization time was longer: 845 ± 22.0 minutes and 815 ± 51.0 minutes, respectively. Furthermore, the 100 nm and crystallization plates with 200 nm iron nano-columns yielded a smaller average number of lysozyme crystals (286 ± 42.0 and 111 ± 26.0 , respectively) than the plate containing 50 nm iron nano-columns (461 ± 83). The size range of the crystals grown on these two platforms are also observed to be significantly larger than the crystals produced on the plate containing iron at a height of 50 nm: 18.0 – 347 μm and 42.0 – 460 μm for 100 nm and 200 nm iron nano-columns, respectively. Figure S4 (Supporting Information) show that one can grow lysozyme crystals

of ~ 100 nm in size after 510 min on 50 nm iron nano-columns deposited crystallization plates. These results demonstrate that the variation of the surface roughness of the iron nano-columns has a significant effect on the number of crystals and no influence on the size of the crystals.

The use of ITO-modified crystallization plates resulted in the growth of lysozyme crystals in the shortest amount of time (370 ± 36 minutes) and the largest size range for lysozyme among each of all the crystallization plates used in this study (56 – 584 μm). These observations can be attributed to the homogenous surface of the ITO film, which provides the largest number of potential nucleation sites for the growth of lysozyme crystals. SEM image of an ITO film in Figure S3 (Supporting Information) shows the rough scratches on the left-hand side of the film were made intentionally to demonstrate the smooth, homogenous nature of the ITO film. It is important to note that all crystallization experiments were carried out on unmodified ITO films and the scratches in Figure S3 are for demonstration purposes only. Figure S5 (Supporting Information) show that one can grow lysozyme crystals of ~ 100 nm in size after 200 min on ITO-modified crystallization plates.

As mentioned earlier in the text, one can use the crystallization plates and the MA-MAEC technique to grow lysozyme crystals of desired size and number by continuously monitoring the growth of crystals using optical microscopy. PMMA is optically transparent visible range of the electromagnetic spectrum allowing optical microscopy studies to be carried out without background interference [27]. To visually compare the efficiency of all crystallization plates for the growth of lysozyme crystals in terms of size, number of crystals, the optical images of lysozyme crystals grown at three different times are given in Figures 2 and 3, where 30 min refers to the time of appearance of measureable crystals, 300 min refer to the time for crystals to reach ~ 100 nm in size and complete crystallization time (i.e., crystals stopped growing). At 30 min, the largest lysozyme crystals were observed on iron nano-columns (200 nm, Figure 3) deposited crystallization plates, where numerous lysozyme crystals of ~ 50 nm with narrow size distribution appeared on the surface of the plates. At 300 min, the largest lysozyme crystals (larger than ~ 100 nm) were observed on both ITO-deposited and iron-columns deposited crystallization plates. In addition, lysozyme crystals reached 90% of their final size at 300 min. At time of complete crystallization, the

largest lysozyme crystals (up to ~460 m) were observed on ITO-modified crystallization plates. Lysozyme crystals with well-defined crystal surfaces appeared in a single well of all crystallization plates. Figures 2 and 3 also demonstrate that continuous microwave heating of the crystallization plates for up to 840 minutes did not cause any damage to the crystallization plates [19].

In addition to the visual comparison of the efficiency of crystallization plates for the growth of lysozyme crystals, XRD crystallography of lysozyme crystals grown on all crystallization plates were carried out, and the results are summarized in Table 2 and Figure S6 (Supporting Information). For the XRD analysis, lysozyme crystals of approximately the same size are chosen from each of the four crystallization plates in order to ensure that a fair comparison is made (each data set were collected at the same crystal-to-detector distance of 120.1 mm with an exposure time of 1 minute, an oscillation angle of 0.5° and an

oscillation range of 61.0°) [23]. Overall, the crystals analyzed yielded excellent diffraction data on all four crystallization plates. Additionally, the indicators of crystal quality (the Rp.i.m. and CC1/2) and average $I/\sigma(I)$ for all resolution shells show diffraction quality lysozyme crystals. The crystals displaying the highest average $I/\sigma(I)$ (27.5 (9.5)) were those grown on the blank plates, while the crystals displaying the lowest average $I/\sigma(I)$ (16.8 (5.5)) were those grown on ITO-modified crystallization plates. It is important to note that the $I/\sigma(I)$ for each of the data sets is excellent and the differences observed are unlikely to affect downstream structure solution, model building, and refinement (data not shown). The average mosaic spread values measure the imperfections in the alignment of individual unit cells within the lysozyme crystals grown on each crystallization plate.

Figure S6 shows low mosaic spread values for the crystals produced on all four crystallization

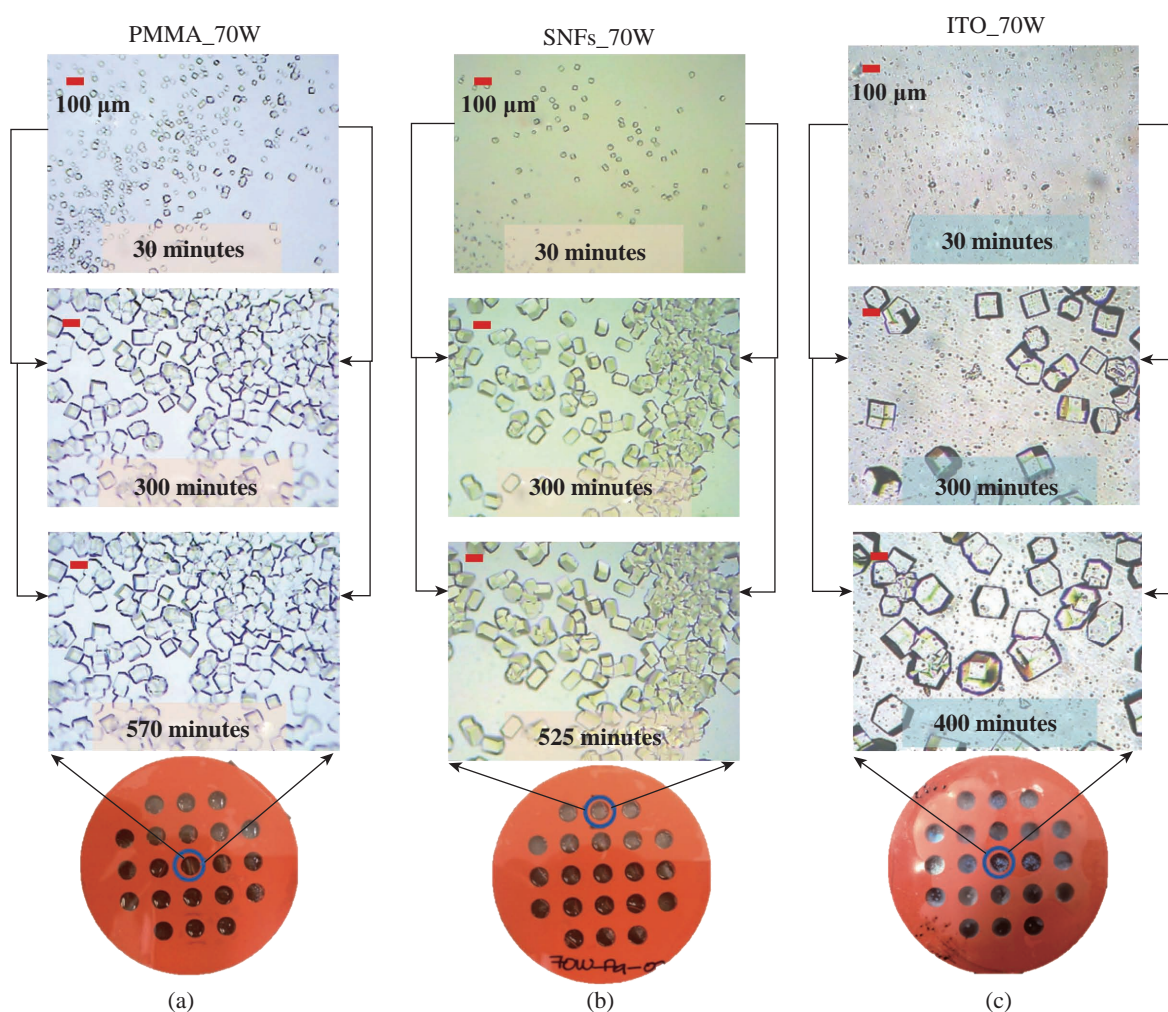


Fig. 2 Optical images of lysozyme crystals formed on (a) blank crystallization plate, (b) SNFs-deposited crystallization plate, (c) ITO-modified crystallization plate at 70 W of power.

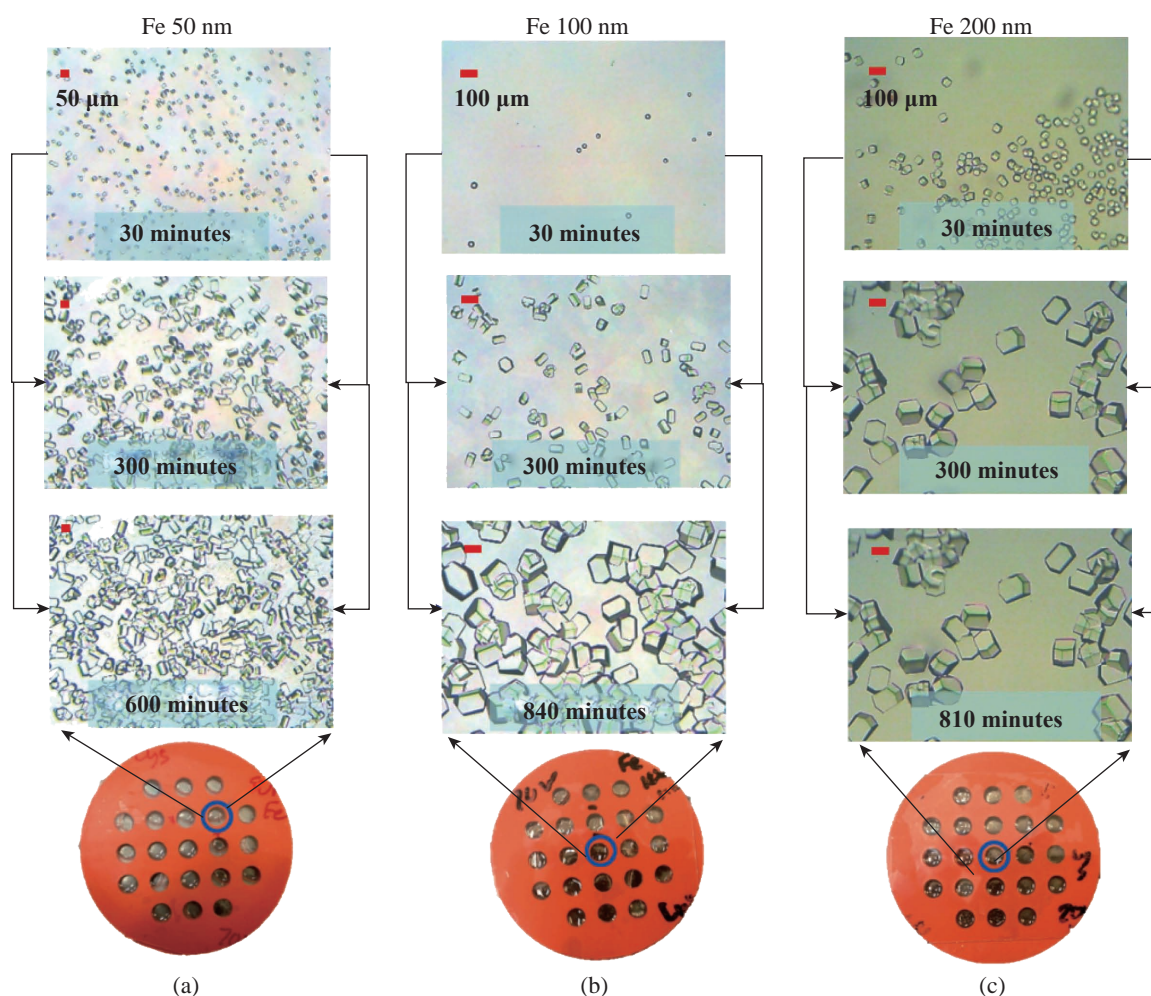


Fig. 3 Optical images of lysozyme crystals formed on iron nano-columns deposited crystallization plates (a) 50 nm iron nano-columns, (b) 100 nm iron nano-columns and (c) 200 nm iron nano-columns at 70 W of microwave heating.

Table 2 X-ray diffraction crystallography data for lysozyme crystals grown on blank crystallization plates, SNFs-deposited crystallization plates, ITO-modified crystallization plates, and iron nano-columns deposited crystallization plates using the iCrystal System at 70 W of microwave power

Crystal	PMMA_70W	Ag_70W	ITO_70W	Fe (50 nm)_70W
Space group	P4 ₃ 2 ₁ 2			
Cell dimension*				
a	77.0	77.15	77.72	77.19
b	77.0	77.15	77.72	77.19
c	37.73	37.77	37.65	37.96
Resolution (Å) [§]	54.45-1.78 (1.81-1.78)	54.55-1.78 (1.81-1.78)	54.45-1.78 (1.81-1.78)	54.59-1.78 (1.81-1.78)
R _{p.i.m.}	0.017 (0.064)	0.025 (0.160)	0.027 (0.086)	0.022 (0.132)
Mean I/s(I)	27.5 (9.5)	19.5 (3.5)	16.8 (5.5)	20.5 (4.6)
CC _{1/2}	0.999 (0.981)	0.999 (0.916)	0.998 (0.969)	0.999 (0.944)
Completeness (%)	81.1 (86.6)	98.1 (99.8)	99.2 (97.5)	99.8 (100.0)
Multiplicity	5.7 (5.2)	4.7 (4.5)	4.6 (4.6)	4.6 (4.5)
Wilson B-factor (Å ²)	13.5	13.8	15.5	16.7
Average mosaicity	0.37	0.42	0.55	0.66

plates, where the largest value (0.66) being observed for crystals grown on the iron nano-columns. The differences between the values for all data sets are also no cause for concern as the differences are small and unlikely to affect downstream structure solution, model building, and refinement (data not shown). These results imply that the iCrystal System is capable of producing crystals of excellent diffraction quality.

Based on the observations described above, ITO-modified crystallization plates are deemed to be the most effective plates for rapid growth of the largest sized lysozyme crystals. Crystallization of lysozyme on ITO-modified crystallization plates were also carried out at room temperature (a control experiment) and the average time for the complete crystallization was recorded as 855 ± 15.0 minutes (Table S2), which is longer than 2-fold for the identical experiment carried out with the MA-MAEC technique (370 ± 36.0 minutes). Although, the size of the lysozyme crystals grown on ITO-modified crystallization plates at room temperature and using the MA-MAEC technique, the average number of crystals grown using the MA-MAEC technique was 2-fold larger than those grown at room temperature. It is also important to demonstrate

the inter-plate variations in the 21-well crystallization plates for the growth of lysozyme crystals. Figures 4 and S7 show the optical images of the lysozyme crystals grown in each of the 21 wells of the ITO-modified crystallization plates using MA-MAEC technique and at room temperature, respectively. Using the MA-MAEC technique, high quality lysozyme crystals were grown on 15 out of 21 wells of the crystallization plate (Figure 4), as compared to 3 out of 21 wells of the crystallization plate at room temperature (Figure S7). Figures 5(a) and 5(b) display the average size distribution of the lysozyme crystals grown on ITO-modified crystallization plates at room temperature and using the MA-MAEC technique, respectively. These figures clearly demonstrate that the use of the ITO films in conjunction with the iCrystal system produces lysozyme crystals that are more abundant and with a relatively narrow size distribution (100-300 nm) than lysozyme crystals produced at room temperature. The observations described above provide strong evidence for superiority of the MA-MAEC technique over the crystallization of lysozyme at room temperature on crystallization plates.

One of the most important criteria for any protein

Lysozyme_ITO_70W

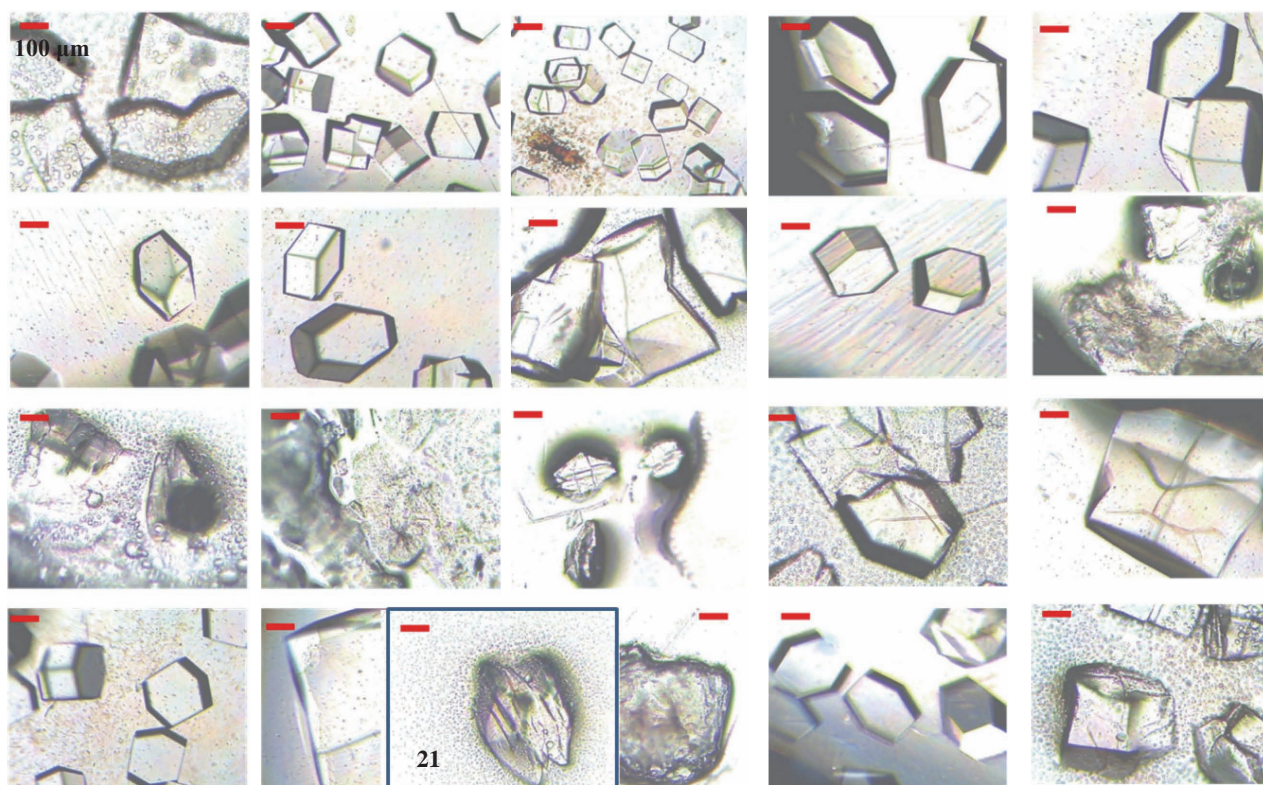


Fig. 4 Optical images of typical lysozyme crystals from each of the 21-wells grown at 70 W on ITO-modified crystallization plates.

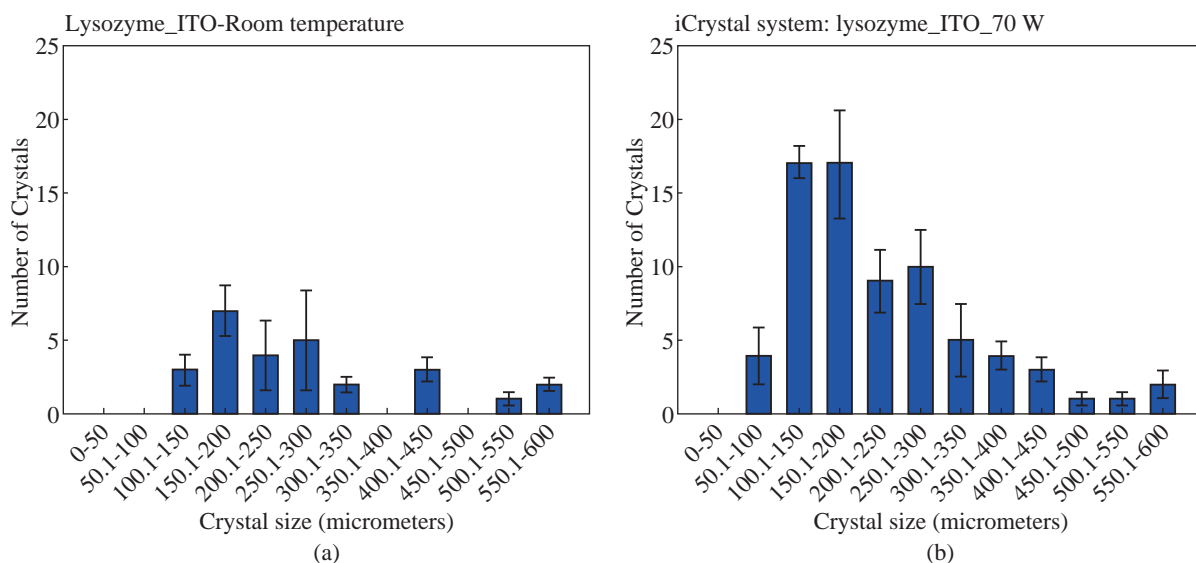


Fig. 5 Crystal size and total number of lysozyme crystals grown at (a) room temperature and at (b) 70 W of microwave heating on ITO-modified crystallization plates.

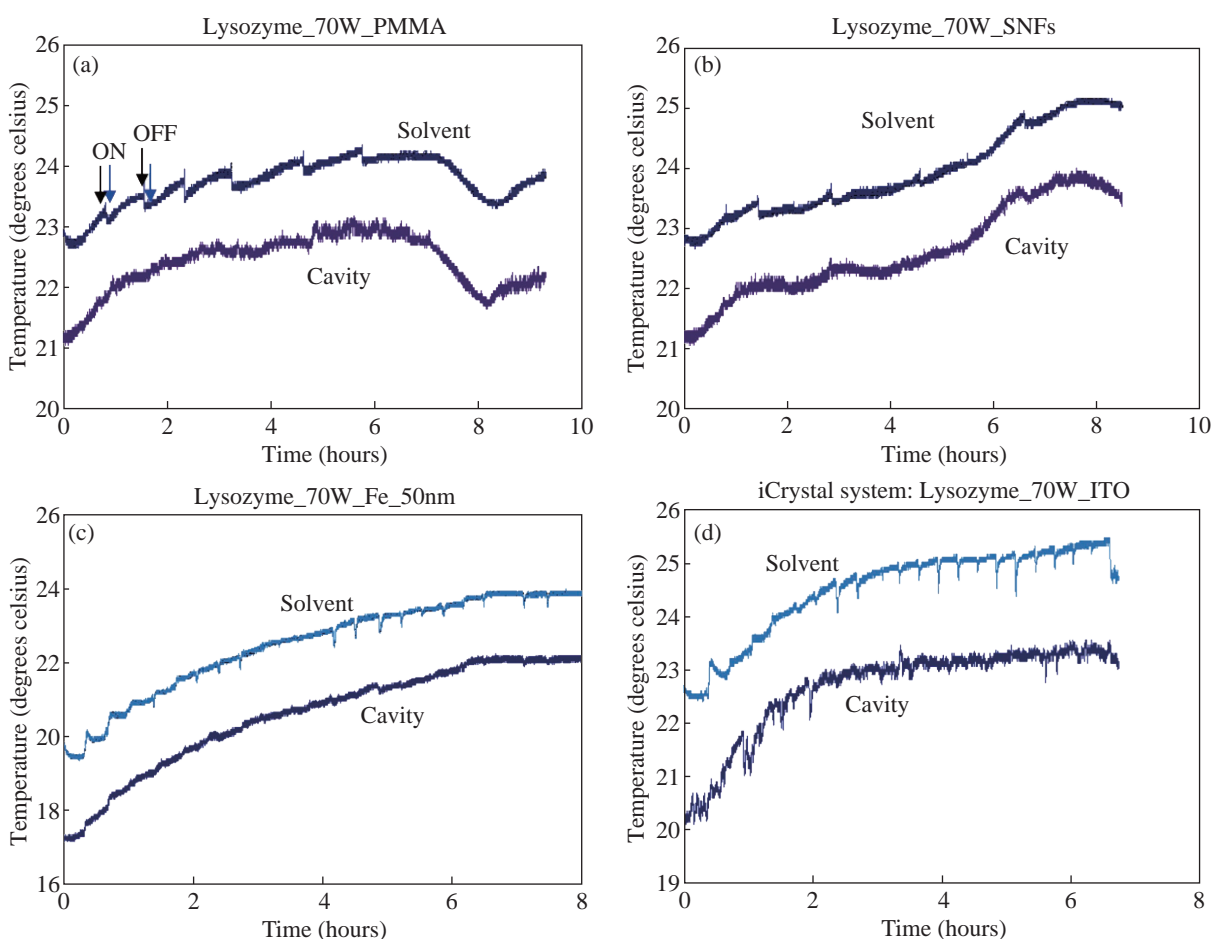


Fig. 6 Real-time temperature of the solvent in a well on a (a) blank crystallization plate, (b) SNFs-deposited crystallization plate, (c) 50 nm iron nano-columns deposited crystallization plate, and (d) ITO-modified crystallization plate measured at 70 W inside the iCrystal system.

crystallization technique is the control over the temperature of the protein solution. Since most proteins

denature above physiological temperatures and the MA-MAEC technique involves microwave heating of

the protein solution, the temperature of the lysozyme solution and the microwave cavity in the iCrystal system was measured. Figure 6 shows the real-time measurements of the temperature of the solvent inside all crystallization plates and the microwave cavity during microwave heating at 70 W. The temperature of both the solvent and the microwave cavity were increased slowly as continuous microwave heating is applied at 15 minute intervals (with 30 sec pause). The temperature of the solvent within the wells was increased steadily over time and to eventually reach a plateau at around 24°C or 25°C when nearing the end of the experiments. The temperature of the cavity was always lower than the solvent in all crystallization experiments, since solvents (and water) absorbs microwave energy more efficiently as compared to air inside the microwave cavity. In addition, since the thermal conductivity values of the metals (silver: 410 W/mK, iron: 55 W/mK, ITO: 12 W/mK) are significantly larger than the thermal conductivity value of the solvent (0.61 W/mK), a thermal gradient is produced between the solvent and the metal surface, which affords for the mass transfer of the proteins from the warmer solvent onto the cooler surface of the metals. Subsequently, the crystallization of proteins can be accelerated on metal surfaces. Our laboratory is currently working on the crystallization of biologically relevant proteins and the results of these studies will be reported in due course.

Conclusions

In this study, crystallization of lysozyme (as a model protein) using four different types of crystallization plates and the MA-MAEC technique in the iCrystal System was investigated. The combination of the MA-MAEC technique with the incorporation of continuous low wattage microwave heating (70 W) facilitated the rapid crystallization of lysozyme on all crystallization plates. The time for complete crystallization was observed to be longest on the blank crystallization plate (555 ± 77 minutes). The shortest crystallization time (370 ± 36 minutes) was observed on the ITO-modified crystallization plates. The use of iron nano-columns afforded for the control over the growth of lysozyme crystals by varying the surface roughness, where the smallest size of lysozyme crystals was observed on iron nano-columns of 50 nm height. Additionally, the blank, SNFs-deposited and iron nano-column deposited crystallization plates yielded

large amounts of lysozyme crystals per plate (a total of 461 crystals on 21-wells of the iron nano-columns of 50 nm height). ITO-modified crystallization plates facilitated the growth of the lysozyme crystals in a significantly shorter amount of time (370 ± 36.0 minutes) as compared all other crystallization plates. The largest lysozyme crystals (up to 460 nm) were grown on ITO-modified crystallization plates. XRD analysis of lysozyme crystals demonstrated that all four crystallization plates can be used to grow high quality lysozyme crystals.

Acknowledgments

Research reported in this publication was partially supported by the National Center for Advancing Translational Sciences of the National Institutes of Health under Award Number R41TR001275. The content is solely the responsibility of the authors and does not necessarily represent the official views of the National Institutes of Health. Additional partial support was provided ARL W911NF-12-2-0041 (Seifu) and from NSF MRI-DMR-1337339 (Seifu).

Supporting Information

Additional information related to optical microscope images and XRD data for lysozyme crystals under experimental conditions not shown in the main text and SEM images of ITO and Fe-modified crystallization plates are provided.

References

- [1] J. Lu, X.J. Wang and C.B. Ching, Batch crystallization of soluble proteins: effect of precipitant, temperature and additive. *Progress in crystal growth and characterization of materials*, 2002, 45: 201-217.
- [2] O. Galkin, P.G. Vekilov, Are nucleation kinetics of protein crystals similar to those of liquid droplets? *Journal of the American Chemical Society*, 2000, 122: 156-163.
- [3] A.M. Alabanza, K. Aslan, Metal-assisted and microwave-accelerated evaporative crystallization: Application to l-alanine. *Crystal growth & design*, 2011, 11: 4300-4304.
- [4] P. Gourdon, J.L. Andersen, K.L. Hein, et al., HiLiDe systematic approach to membrane protein crystallization in lipid and detergent. *Crystal growth & design*, 2011, 11: 2098-2106.
- [5] B. Zheng, L.S. Roach and R.F. Ismagilov, Screening of protein crystallization conditions on a microfluidic chip using nanoliter-size droplets. *Journal of the American chemical society*, 2003, 125: 11170-11171.
- [6] A. D'arcy, A. Mac Sweeney and A. Haber, Practical aspects of using the microbatch method in screening conditions for protein crystallization. *Methods*, 2004, 34: 323-328.

- [7] J.K. Baird, J.C. Clunie, Kinetics of lysozyme crystallization from solution. *Physics and Chemistry of Liquids*, 1999, 37: 285-295.
- [8] C.M. Niemeyer, Nanoparticles, proteins, and nucleic acids: biotechnology meets materials science. *Angewandte Chemie International Edition*, 2001, 40: 4128-4158.
- [9] S. Fermani, G. Falini, M. Minnucci, et al., Protein crystallization on polymeric film surfaces. *Journal of crystal growth*, 2001, 224: 327-334.
- [10] A. Garcia-Caballero, J.A. Gavira, E. Pineda-Molina, et al., Optimization of protein crystallization: The OptiCryst project. *Crystal Growth & Design*, 2011, 11: 2112-2121.
- [11] A.Y. Lee, I.S. Lee, S.S. Dette, et al., Crystallization on confined engineered surfaces: a method to control crystal size and generate different polymorphs. *J Am Chem Soc*, 2005, 127: 14982-14983.
- [12] J.J. Gray, The interaction of proteins with solid surfaces. *Current opinion in structural biology*, 2004, 14: 110-115.
- [13] S. Khurshid, E. Saridakis, L. Govada, et al., Porous nucleating agents for protein crystallization. *Nat. Protocols*, 2014, 9: 1621-1633.
- [14] T.M. Young, C.J. Roberts, Structure and thermodynamics of colloidal protein cluster formation: Comparison of square-well and simple dipolar models. *The Journal of chemical physics*, 2009, 131: 125104.
- [15] M.A. Blanco, E. Sahin, A.S. Robinson, et al., Coarse-Grained Model for Colloidal Protein Interactions, B 22, and Protein Cluster Formation. *The Journal of Physical Chemistry B*, 2013, 117: 16013-16028.
- [16] M.A. Martí-Renom, A.C. Stuart, A. Fiser, et al., Comparative protein structure modeling of genes and genomes. *Annual review of biophysics and biomolecular structure*, 2000, 29: 291-325.
- [17] M.A. Pinard, K. Aslan, Metal-assisted and microwave-accelerated evaporative crystallization. *Crystal growth & design*, 2010, 10: 4706-4709.
- [18] A.M. Alabanza, E. Pozharski and K. Aslan, Rapid crystallization of l-alanine on engineered surfaces by use of metal-assisted and microwave-accelerated evaporative crystallization. *Crystal growth & design*, 2011, 12: 346-353.
- [19] M. Mohammed, M.F. Syed, M.J. Bhatt, et al., Rapid and selective crystallization of acetaminophen using metal-assisted and microwave-accelerated evaporative crystallization. *Nano biomedicine and engineering*, 2012, 4: 35.
- [20] A.M. Alabanza, M. Mohammed and K. Aslan, Crystallization of amino acids on a 21-well circular PMMA platform using metal-assisted and microwave-accelerated evaporative crystallization. *Nano Biomed Eng*, 2013, 5: 140-147.
- [21] A. Mojibola, G. Dongmo-Momo, M. Mohammed, et al., Crystal engineering of l-alanine with l-leucine additive using metal-assisted and microwave-accelerated evaporative crystallization. *Cryst Growth Des*, 2014, 14: 2494-2501.
- [22] K. Mauge-Lewis, A. Mojibola, E.A. Toth, et al., Metal-assisted and microwave-accelerated evaporative crystallization: proof-of-principle application to proteins. *Crystal Growth & Design*, 2015,
- [23] T.G.G. Battye, L. Kontogiannis, O. Johnson, et al., iMOSFLM: a new graphical interface for diffraction-image processing with MOSFLM. *Acta Crystallographica Section D: Biological Crystallography*, 2011, 67: 271-281.
- [24] P.R. Evans, An introduction to data reduction: space-group determination, scaling and intensity statistics. *Acta Crystallographica Section D: Biological Crystallography*, 2011, 67: 282-292.
- [25] M.D. Winn, C.C. Ballard, K.D. Cowtan, et al., Overview of the CCP4 suite and current developments. *Acta Crystallographica Section D: Biological Crystallography*, 2011, 67: 235-242.
- [26] A.M. Alabanza, M. Mohammed and K. Aslan, Crystallization of l-alanine in the presence of additives on a circular PMMA platform designed for metal-assisted and microwave-accelerated evaporative crystallization. *Cryst Eng Comm*, 2012, 14: 8424-8431.

Copyright© 2016 Kevin Mauge-Lewis, Brittney Gordon, Fareeha Syed, Saarah Syed, Enock Bonyi, Muzaffer Mohammed, Eric A. Toth, Dereje Seifu, and Kadir Aslan. This is an open-access article distributed under the terms of the Creative Commons Attribution License, which permits unrestricted use, distribution, and reproduction in any medium, provided the original author and source are credited.